Topographically Distinct Epidermal Nociceptive Circuits Revealed by Axonal Tracers Targeted to *Mrgprd*

Mark J. Zylka, Frank L. Rice and David J. Anderson

Supplemental Experimental Procedures

Molecular Biology

To determine the gene structure of mouse *Mrgprd*, we performed 5′ and 3′ RACE reactions (Smart RACE cDNA Amplification Kit, Clontech) using poly-A RNA isolated from adult mouse trigeminal ganglia. The full-length *Mrgprd* cDNA sequence was deposited as GenBank accession number AY762266.

The arms of the *Mrgprd* targeting constructs were subcloned from a 129/SvJ genomic DNA BAC clone (Genome Systems). The gene deletion constructs eliminated amino acids 20 to 315 from the 321 amino acid coding region of MRGPRD (GenBank accession number AAK91800). EGFPf (Clontech) and a genomic fragment of PLAP were ligated in-frame to a preexisting NcoI site located 19 amino acids downstream from the start codon. To create the gene-conserving construct, IRES-EGFPf-rtTA2(S)M2-ACN was ligated into an AscI restriction site engineered immediately 3′ of the *Mrgprd* stop codon. All constructs contained the EMCV IRES (Mountford et al., 1994) followed by rtTA2(S)M2 (Urlinger et al., 2000) and a self-excising loxP-flanked pol-II promoter-neomycin resistance cassette (ACN) (Bunting et al., 1999). Homologous recombination was performed in mouse CJ7 embryonic stem (ES) cells following standard procedures. Correctly targeted ES cell clones were identified by Southern blot hybridization using probes that flanked the 5′ and 3′ arms of the targeting constructs, as well as an internal neomycin probe. Chimeric mice were produced by blastocyst injection and were mated to C57Bl/6 mice to establish lines. In all cases, loss of the ACN selection cassette was confirmed by PCR. *Mrgprd* homozygous knockout mice are viable and show no obvious phenotypic or behavioral abnormalities. Tissue was obtained from mice that were backcrossed to C57Bl/6 mice for two or five generations.

Immunofluorescence

Adult mice, ages 6–12 weeks, were anesthetized with pentobarbital and perfused transcardially with 20 ml 0.9% saline (4°C) followed by 25 ml fixative (4% formaldehyde, 14% [v/v] sat. picric acid, 0.1 M phosphate buffer [pH 7.3] at 4°C). Mystacial pads, spinal cord encompassing the lumbar enlargement (L4-L6 region), and all peripheral tissues (except DRG and glabrous skin) were carefully dissected and postfixed for 2 hr at 4°C in the same fixative. L4-L6 DRG from perfused animals were postfixed for 5 min at 4°C. Newborn mice were anesthetized by being placed on an ice water slurry until motionless, then were perfused transcardially with 2 ml 0.9% saline (4°C) followed by 4 ml of the fixative described above. All tissues were cryoprotected in 20% sucrose, 0.1 M phosphate buffer (pH 7.3) at 4°C for 24 hr, frozen in OCT, sectioned with a cryostat at 20 μm, and mounted on Superfrost Plus slides. Slides were stored at −20°C.

Glabrous skin was dissected from the hindpaws of nonperfused adult mice, then immersion fixed for 18 hr at 4°C in Zamboni's fixative (2% formaldehyde, 15% [v/v] sat. picric acid, 0.1 M phosphate buffer [pH 7.3]), cryoprotected, and frozen in OCT, as described (Navarro et al., 1995). This fixation method yielded substantially stronger epidermal CGRP staining when compared to perfused tissue. Glabrous tissue was sectioned at 30 μm and placed directly in PBS with 0.1% Triton X-100 (PBS+TX) for immediate staining as free-floating sections.

Frozen slides were dried at 35°C for 15 min and then fixed in 4% formaldehyde in PBS for 10 min. Free-floating and slide-mounted sections were washed three times with PBS+TX, blocked for 30 min in PBS+TX containing 10% goat serum and 5% donkey serum—if donkey secondary antibodies were also used—then incubated overnight at 4°C with primary antibodies diluted in blocking solution. We used 1:1000 rabbit anti-GFP (A-11122; Molecular Probes), 1:1000 chicken anti-GFP (GFP-1020; Aves Labs), 1:200 mouse anti-human PLAP (clone 8B6; DAKO), 1:800 guinea pig anti-CGRP (T-5027; Peninsula), 1:1000 rabbit anti-CGRP (T-4239; Peninsula), 1:1000 rabbit anti-human PGP 9.5 (Ultraclone), 1:1000 rabbit anti-NF200 (AB1982; Chemicon), 1:1000 rabbit anti-P2X3 (AB5895; Chemicon), 1:1000 rabbit anti-peripherin (AB1530; Chemicon), 1:4 Armenian hamster anti-c-RET (Lo and Anderson, 1995), 1:200 rabbit anti-Trpv1 (PC420; Oncogene Research Products), 1:100 mouse anti-PKCγ (clone PKC66; Cat. #13-3800; Zymed), 1:1000 rabbit anti-PKCγ (c-19; Cat. #sc-211; Santa Cruz Biotechnology). Sections were then washed three times with PBS+TX and incubated for 2 hr at room temperature with secondary antibodies. All secondary antibodies were diluted 1:250 in blocking solution and were conjugated to Alexa-488, Alexa-568, or Alexa-633 fluorochromes (Molecular Probes), or to FITC, Cy3, or Cy5 fluorochromes (Jackson ImmunoResearch). To detect IB4 binding, we included 1:80 *Griffonia simplicifolia* isolectin GS-IB_4-Alexa 568 (I-21412; Molecular Probes) during secondary antibody incubations. Nuclei were counterstained with TO-PRO-3 (Molecular Probes). Sections were washed three times with PBS+TX and wet-mounted in Gel/Mount (Biomeda). Images were obtained using a Leica TCS-NT confocal microscope system.

Quantification

Four to ten confocal images (~2 μm optical thickness) from heterozygous mice and from homozygous mice were counted to quantify the percentage of *Mrgprd*$^+$ L4-L6 DRG neurons that coexpressed a given nociceptive marker. Paired Student's t tests were performed to determine if there were differences between genotypes.

To quantify free nerve fibers, confocal images (merged image stack was 20–30 μm and made up of many 0.5–2 μm optical sections, using a Leica HCX PL APO 40×/1.25–0.75 oil lens) were taken from random regions of thin (dermal papillae-lacking) and thick (dermal papillae-containing) glabrous skin. At least 200 fibers were imaged per genotype. Within each image, the number of *Mrgprd*$^+$ fibers was scored as a percentage of all fibers in the image (relative to CGRP or PGP 9.5). Paired Student's t tests were performed to determine if there were differences between genotypes.

PLAP Histochemistry

Tissue was procured from perfused adult mice and sectioned as described above. Sections were dried on Superfrost Plus slides at 35°C for 15 min, postfixed in 4% formaldehyde in PBS for 10 min, washed three times with Hank's balanced salt solution (HBSS; Gibco; Cat. #14025-092), incubated at 65°C for 2–6 hr in HBSS, washed three times with HBSS, then washed twice in alkaline phosphatase (AP) buffer (0.1 M Tris [pH 9.5], 0.1 M NaCl, 50 mM $MgCl_2$, 0.1% Tween-20, 5 mM levamisole-added fresh). PLAP activity was then visualized by incubating sections in 37.5 μg/ml nitro blue tetrazolium, 175 μg/ml 5-bromo-4-chloro-3-indolyl phosphate in AP buffer at room temperature overnight and protected from light.

Electron Microscopy

Homozygous *Mrgprd*Δ^{PLAP} mice were anesthetized and perfused with 4% formaldehyde, 0.05% glutaraldehyde, 0.1 M phosphate buffer (pH 7.3). Sciatic nerves were removed, postfixed for 2 hr at 4°C, cryoprotected overnight at 4°C (20% sucrose, 0.1 M phosphate buffer [pH 7.3]), frozen in OCT, and sectioned at 40 μm lengthwise using a cryostat. Free-floating sections were heated

at 65°C for 2 hr to inactivate endogenous phosphatases, then PLAP activity was visualized by precipitating electron-dense cerium phosphate, based on the "oCPP" method (Radcke et al., 2002). We modified preincubation buffer 2 (50 mM Tricine, 30% sucrose, 3.9 mM $MgSO_4$, 50 mM diethanolamine, 0.1% Tween-20 [pH 9.5]) and carried out the cerium precipitation reaction at 37°C for 6.5 hr.

After oxidation of Ce(III) to Ce(IV), the sections were postfixed in 2% glutaraldehyde followed by osmium tetroxide (1% OsO_4, 0.1 M cacodylate, 1.8 mM $CaCl_2$, 0.8 mM $MgSO_4$ [pH 7.4]), counterstained en bloc with 1% uranyl acetate and 0.4% lead citrate, and embedded in Epon. Transverse ultrathin sections were cut, mounted on formvar-coated slot grids, and imaged using a Philips 420 transmission electron microscope.

Supplemental References

S1. Bunting, M., Bernstein, K.E., Greer, J.M., Capecchi, M.R., and Thomas, K.R. (1999). Targeting genes for self-excision in the germ line. Genes Dev. *13*, 1524–1528.

S2. Chess, A., Simon, I., Cedar, H., and Axel, R. (1994). Allelic inactivation regulates olfactory receptor gene expression. Cell *78*, 823–834.

S3. Fundin, B.T., Silos-Santiago, I., Ernfors, P., Fagan, A.M., Aldskogius, H., DeChiara, T.M., Phillips, H.S., Barbacid, M., Yancopoulos, G.D., and Rice, F.L. (1997). Differential dependency of cutaneous mechanoreceptors on neurotrophins, trk receptors, and P75 LNGFR. Dev. Biol. *190*, 94–116.

S4. Khodorova, A., Navarro, B., Jouaville, L.S., Murphy, J.E., Rice, F.L., Mazurkiewicz, J.E., Long-Woodward, D., Stoffel, M., Strichartz, G.R., Yukhananov, R., and Davar, G. (2003). Endothelin-B receptor activation triggers an endogenous analgesic cascade at sites of peripheral injury. Nat. Med. *9*, 1055–1061.

S5. Lo, L., and Anderson, D.J. (1995). Postmigratory neural crest cells expressing c-RET display restricted developmental and proliferative capacities. Neuron *15*, 527–539.

S6. Mountford, P., Zevnik, B., Duwel, A., Nichols, J., Li, M., Dani, C., Robertson, M., Chambers, I., and Smith, A. (1994). Dicistronic targeting constructs: reporters and modifiers of mammalian gene expression. Proc. Natl. Acad. Sci. USA *91*, 4303–4307.

S7. Navarro, X., Verdu, E., Wendelscafer-Crabb, G., and Kennedy, W.R. (1995). Innervation of cutaneous structures in the mouse hind paw: a confocal microscopy immunohistochemical study. J. Neurosci. Res. *41*, 111–120.

S8. Radcke, C., Stroh, T., Dworkowski, F., and Veh, R.W. (2002). Specific visualization of precipitated cerium by energy-filtered transmission electron microscopy for detection of alkaline phosphatase in immunoenzymatic double labeling of tyrosine hydroxylase and serotonin in the rat olfactory bulb. Histochem. Cell Biol. *118*, 459–472.

S9. Rice, F.L., Albers, K.M., Davis, B.M., Silos-Santiago, I., Wilkinson, G.A., LeMaster, A.M., Ernfors, P., Smeyne, R.J., Aldskogius, H., Phillips, H.S., et al. (1998). Differential dependency of unmyelinated and Aδ epidermal and upper dermal innervation on neurotrophins, trk receptors, and $p75^{LNGFR}$. Dev. Biol. *198*, 57–81.

S10. Rodriguez, I., Feinstein, P., and Mombaerts, P. (1999). Variable patterns of axonal projections of sensory neurons in the mouse vomeronasal system. Cell *97*, 199–208.

S11. Urlinger, S., Baron, U., Thellmann, M., Hasan, M.T., Bujard, H., and Hillen, W. (2000). Exploring the sequence space for tetracycline-dependent transcriptional activators: novel mutations yield expanded range and sensitivity. Proc. Natl. Acad. Sci. USA *97*, 7963–7968.

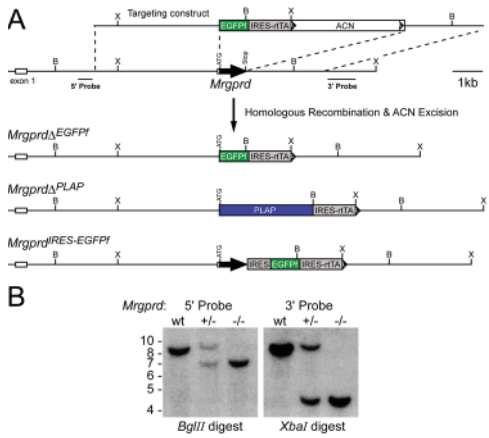

Figure S1. Targeting Axonal Tracers to *Mrgprd*

(A) A targeting construct was designed to replace the entire coding region of *Mrgprd*, located within the second exon, with EGFPf followed by the encephalomyocarditis (EMCV) internal ribosomal entry site (IRES), the reverse tetracycline transactivator (rtTA; version rtTA2(S)M2 [Urlinger et al., 2000]), and the self-excising, loxP-flanked, neomycin resistance cassette (ACN; Bunting et al., 1999). After homologous recombination and passage through the male germline, the ACN cassette was self-excised, leaving behind a single loxP site ("L"). *Mrgprd* gene deletion (*Mrgprd*Δ^{PLAP}) and *Mrgprd* gene-conserving (*Mrgprd*$^{IRES\text{-}EGFPf}$) knockin mouse lines were also generated. "B," BglII; "X," XbaI.

(B) Liver genomic DNA from wild-type (wt), heterozygous (+/–) and homozygous (–/–) *Mrgprd*Δ^{EGFPf} mice was Southern blotted and hybridized with probes (shown in [A]) that flank the targeting constructs to confirm homologous recombination.

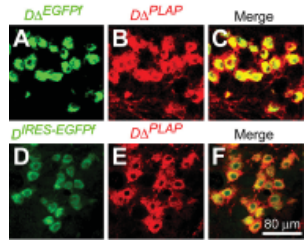

Figure S2. Biallelic Expression of *Mrgprd*

(A–C) All DRG neurons coexpress EGFPf (green) and PLAP (red) in mice bearing the gene-deleting alleles *Mrgprd*Δ^{EGFPf} and *Mrgprd*Δ^{PLAP}, or (D–F) one gene-conserving (*Mrgprd*$^{IRES\text{-}EGFPf}$) and one gene-deleting (*Mrgprd*Δ^{PLAP}) allele. Each neuron has a rim of red stain (PLAP) that does not overlap with EGFPf (C and F). This is due to the fact that PLAP is localized to the extracellular face of the plasma membrane, whereas EGFPf is localized to the cytoplasmic face. Both markers also diffusely stain the cytoplasm because they are localized to intracellular membrane compartments. Note that the EGFPf staining intensity is weaker in (D) compared to (A) because of significantly reduced translation following the IRES sequence. Scale bar is the same for all images.

These data indicated that both markers show equal expressivity and that the *Mrgprd* gene is biallelically expressed, regardless of whether the *Mrgprd* coding sequence is deleted or conserved. Thus, unlike the case for members of other large GPCR families, *Mrgprd* is not expressed monoallelically (Chess et al., 1994; Rodriguez et al., 1999) or imprinted. Since all *Mrgprd*$^+$ neurons can express both a functional and a nonfunctional allele (F), individual cells in heterozygous *Mrgprd*$^{EGFPf/+}$ or *Mrgprd*$^{PLAP/+}$ mice should be phenotypically wild-type for *Mrgprd* function. Consistent with this assumption, we observed no obvious differences in the marker profile or projections (see text) of *Mrgprd*-expressing neurons from heterozygous or homozygous *Mrgprd*^{EGFPf} or *Mrgprd*^{PLAP} mice. Moreover, the fact that the gene-conserving EGFPf reporter is similarly expressed, qualitatively, as is the gene-replacing EGFPf reporter, argues against haploinsufficiency for *Mrgprd* function.

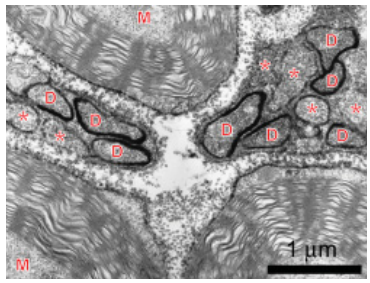

Figure S3. *Mrgprd*-Expressing Neurons Exclusively Have Unmyelinated Axons

Transverse section of the sciatic nerve from *Mrgprd*Δ^{PLAP} stained for PLAP activity by precipitating cerium phosphate. Electron microscopic analysis revealed a dense precipitate on the plasma membranes of unmyelinated, small-diameter, *Mrgprd*$^+$ axons ("D"). *Mrgprd*$^+$ axons were bundled together with unstained, small-diameter unmyelinated axons ("*"). These bundles were enveloped by Schwann cell processes. Myelinated axons ("M") were not *Mrgprd*$^+$. Although the electron-dense PLAP reaction product did not precipitate on *Mrgprd*$^+$ nerve fibers in the epidermis, the bundling of *Mrgprd*$^+$ fibers with *Mrgprd*-negative fibers observed in the sciatic nerve is consistent with the intertwining in epidermis observed by confocal microscopy.

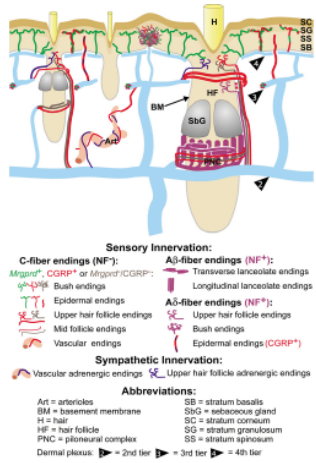

Figure S4. Summary of Innervation in Hairy Skin (Intervibrissal Fur) of the Mouse

Includes our current findings in relationship to previous studies of innervation within mouse skin (Fundin et al., 1997; Rice et al., 1998). As in glabrous skin, *Mrgprd*$^+$ fibers were occasionally intertwined with CGRP$^+$ fibers within the epidermis. Most *Mrgprd*$^+$ fibers terminated as penicillate endings in the epidermis or as penetrating endings within the upper epidermal necks of hair follicles. In rare cases, we could not conclusively determine if *Mrgprd* and CGRP fibers were intertwined or if these markers were in the same fiber (red and green striped fibers). The stratum granulosum is differentially shaded to highlight the approximate, suprabasal, location of β-endorphin (Khodorova et al., 2003)

Table S1. Axonal Projections in *Mrgprd*^{EGFPf} and *Mrgprd*^{PLAP} Knockout Mice*

Tissue[a]	Axons Present	Tissue[a]	Axons Present
Sensory		**Viscera**	
Dorsal root ganglia	+	Bladder	–
Trigeminal ganglia	+	Blood vessels	–
Spinal cord	+	Brown fat	–
Sympathetic ganglia	–	Esophagus	–
		Heart	–
Skin		Intestine, large	–
Unmyelinated endings:		Intestine, small	–
Epidermal free nerve endings	+	Joints, perosteum	–
Bush/cluster endings	+	Kidney	–
Circular follicle neck endings	+	Liver	–
Penetrating follicle neck endings	+	Lung	–
Circumferential free nerve endings	+ (very rare)	Skeletal muscle	–[c]
		Smooth muscle	–
Myelinated Endings:		Testis	–
Lanceolate/club endings	–		
Merkel cells and endings	–	**Brain**	
Meissner's corpuscles	–	Amygdala	–
		Brainstem-nucleus caudalis	+
Mixed/Other		Brainstem—all other areas	–
Blood vessels/vascular endings	–/+[b]	Cerebellum	–
Skeletal muscle	–	Cerebral cortex	–
Sweat glands	–	Hippocampus	–
		Hypothalamus	–
Additional Tissues		Meninges	–
Eye-cornea	–	Olfactory bulb	–
Eye-retina	–	Septum	–
Tongue	–	Striatum	–
		Thalamus	–

*Projections were the same in heterozygous and homozygous gene deletion mice.

[a]Of all these tissues, Mrgprd-EGFPf or Mrgprd-PLAP cell body staining was detected only in DRG and trigeminal ganglia. Furthermore, Mrgprd probes did not hybridize to commercial (Clontech) Northern blots containing polyadenylated RNA from the following mouse tissues: heart, brain, spleen, lung, liver, skeletal muscle, kidney, testis, large intestine, prostate, stomach, thyroid, thymus, salivary glands, uterus. Taken together, these data indicated that Mrgprd was exclusively expressed in nociceptive neurons and not expressed in other body tissues.

[b]Mrgprd+ axons innervate some deep dermal/hypodermal blood vessels in newborns; in the adult, Mrgprd+ fibers rarely innervate deep dermal/hypodermal blood vessels.

[c]Mrgprd+ axons were observed in fiber bundles coursing through muscle. Mrgprd+ axons did not innervate muscle parenchyma.